Pseudo-Spectral Method for the Modelling of Quantization Effects in Nanoscale MOS Transistors

Alan Paussa*, Francesco Conzatti*, Dimitri Breda†, Rossana Vermiglio† and David Esseni*
*DIEGM, University of Udine, Via delle Scienze 208, 33100 Udine, Italy, Fax:+39-0432-558251
†DIMI, University of Udine, Via delle Scienze 208, 33100 Udine, Italy
Email: esseni@uniud.it

***Abstract*— This paper presents a systematic comparison between the numerical efficiency of the pseudo-spectral (PS) and finite difference (FD) methods for the solution of eigenvalue problems related to both n and p-MOS transistors, with different geometries and carrier dimensionalities. Our results indicate remarkable advantages of the PS compared to the FD method in terms of CPU time.**

I. Introduction

The numerical solution of eigenvalue problems is a crucial step in the modelling of nano-structured devices, which is most frequently addressed by using the finite difference (FD) or the finite element method. Recent investigations, however, have pointed out the potentials of the pseudo-spectral (PS) method (for a 1D effective mass Schrödinger equation in electron inversion layers [1], [2]) and of the spectral element method (for the 3D effective mass Schrödinger equation [3], [4]). This paper presents a systematic comparison between PS and FD numerical efficiency for eigenvalue problems related to both n and p-MOS transistors, obtained by implementing with both approaches a self-consistent Schrödinger-Poisson solver for: (a) the 1D quantization problem in p-MOSFETs with the six-by-six $\mathbf{k}\cdot\mathbf{p}$ Hamiltonian; (b) the 2D effective mass Schrödinger equation in cartesian coordinates for n-type FinFETs or rectangular nanowires; (c) the 2D Schrödinger equation in polar coordinates for cylindrical nanowires.

II. Pseudo-spectral method

The PS method for a differential problem approximates the unknown function by using algebraic polynomials in cartesian coordinates and trigonometric polynomials in polar coordinates. If the unknown function is smoothly varying in the real space, then the PS method can achieve the *spectral accuracy*, which consists in an exponential reduction of the approximation error according to c^N (with N being the degree of the polynomial and $c \in (0,1)$), that results in a much faster error reduction with respect to the second order FD approach. Considering a 1D example, the unknown function $u(x)$, with $x \in [0, L]$, can be approximated by the N-degree algebraic polynomial defined in the Lagrange form as

$$u(x) \approx \sum_{j=0}^{N} \ell_j(x) u(x_j) \qquad (1)$$

where the x_j are the Chebyshev extremal nodes [5]:

$$x_j = 0.5\, L \left[1 + \cos\left(\frac{j\pi}{N}\right)\right] \text{with } \; j = 0, 1, \ldots N \qquad (2)$$

and $u_j{=}u(x_j)$ are the unknown values of $u(x)$ at x_j. The functions $l_j(x)$ are the Lagrange basis polynomials of degree N defined as [6]:

$$\ell_j(x) = \prod_{i=0,\, i\neq j}^{N} \frac{x - x_i}{x_j - x_i} \text{with } \; j = 0, 1, \ldots N \qquad (3)$$

In the PS approach the derivatives of $u(x)$ at the nodes x_j are approximated with those of the approximating polynomial defined in Eq.1. Thus, any differential problem or eigenvalue differential problem can be converted to an algebraic problem, whose unknowns are the $u(x_j)$ values. It is worth noting that, differently from the FD method, the discretization matrices for the PS method are not sparse. However, as it will be shown in Sec.IV, the remarkable reduction of the number of discretization points allowed for by the PS with respect to the FD method results in an overall decrease of the CPU time. It should be also pointed out that the calculation of any integral over the interval [0,L] involving the function $u(x)$ can be approximated by an integral of the Lagrange polynomials $\ell_j(x)$.

For a periodic function $u(\theta)$, the trigonometric polynomials defined over a grid of equispaced points allow a better approximation with respect to algebraic polynomials [5]; such an approximation results in a Fourier series expansion. Both the basic definitions and the properties of PS method are extended quite-naturally to multi-dimensional cases.

In order to achieve the spectral accuracy even in problems where the unknown function has discontinuous derivatives (e.g. electrostatic potential over non-homogeneous materials), we have employed one interpolating polynomial for each sub-domain where the unknown function is regular, with the appropriate continuity conditions at the boundaries between different sub-domains.

III. Quantization problems

The first application of the PS method considered in this work is the 1D quantization problem in p-MOS transistors

978-1-4244-7700-5/10/$26.00 ©2010 IEEE

described by the six-by-six **k·p** Hamiltonian as [7], [8]:

$$\left[\hat{\mathbf{H}}_{\mathbf{k}\cdot\mathbf{p}}\left(\mathbf{k},-i\frac{\partial}{\partial z}\right)+\mathbf{H}_{so}+\mathbf{I}\,U(z)\right]\boldsymbol{\xi}_{n,\mathbf{k}}(z)= \\ =E_n(\mathbf{k})\,\boldsymbol{\xi}_{n,\mathbf{k}}(z), \tag{4}$$

where $\boldsymbol{\xi}_{n,\mathbf{k}}(z)$ is a six components wave-function taking complex values, $U(z)$ is the confining potential energy for holes, **I** is the six-by-six identity matrix and $E_n(\mathbf{k})$ is the eigenvalue corresponding to wave-vector $\mathbf{k}=(k_x,k_y)$ in the transport plane. The spin orbit Hamiltonian $\mathbf{H}_{so}$ is a **k** independent matrix. The definition of the **k·p** Hamiltonian operator $\hat{\mathbf{H}}_{\mathbf{k}\cdot\mathbf{p}}$ can be found in [8]. Solving the eigenvalue problem in Eq.4 is well known to be computationally demanding because the wave-functions are six components vectorial functions and, furthermore, the energy dispersion has to be obtained by varying the wave-vector **k** as a parameter of the Hamiltonian [8].

The second benchmark problem is the 2D Schrödinger equation stemming from the effective mass approximation (EMA) model for the electron energy calculation; the problem is relevant for both narrow FinFETs and nanowires. Following [9], the EMA quantization model leads to a 2D Schrödinger equation in the quantization plane (y,z) normal to the transport direction x. By denoting with $\sigma_{\nu,j}(y,z)$ and $\varepsilon_{\nu,j}$ the wave-function and the energy minimum of the valley ν and subband j, the electron energy is finally given by

$$E_{\nu,j}(k_x)=\varepsilon_{\nu,j}+\frac{\hbar^2k_x^2}{2m_x} \tag{5}$$

with m_x being the transport mass (see Tab.1).

As a third case study, we considered cylindrical nanowires described by using the polar coordinates (r,θ) in the (y,z) plane. By expressing the differential operators in polar coordinates, the EMA Schrödinger equation reads

$$-\frac{\hbar^2}{2}\left[w_1\frac{\partial^2\sigma_{\nu,j}}{\partial r^2}+w_2\frac{\partial\sigma_{\nu,j}}{\partial r}+w_3\frac{\partial^2\sigma_{\nu,j}}{\partial r\partial\theta}+w_4\frac{\partial\sigma_{\nu,j}}{\partial\theta}+ \\ +w_5\frac{\partial^2\sigma_{\nu,j}}{\partial\theta^2}\right]+U(r,\theta)\;\sigma_{\nu,j}=\varepsilon_{\nu,j}\;\sigma_{\nu,j} \tag{6}$$

The r and θ dependent coefficients w_i and the transport mass m_x are given in Tab.I for the silicon Δ valleys and the (100) transport direction. It should be emphasized that for the lowest valleys (i.e. ν=1 and 2 in Tab.I) Eq.6 has no radial symmetry, because m_t and m_l are very different for silicon.

The PS approach for polar coordinates was employed by combining Chebyshev expansion in the radial coordinate r with Fourier expansion in the angular coordinate θ. The singularity at r=0 of Eq.6 (see the w_i expressed in Tab.I) was avoided by following the so-called *diameter approach* (see for details [5]). For all the quantization problems described above we developed a self-consistent solver of the Schrödinger-Poisson equations.

TABLE I

PARAMETERS OF EQ.6 FOR THE SILICON Δ VALLEYS AND THE [100] TRANSPORT DIRECTION (m_t=0.19m_0 AND m_l=0.92m_0 ARE THE TRANSVERSE AND LONGITUDINAL EFFECTIVE MASSES).

	ν=1	ν=2	ν=3
g_ν	2	2	2
w_1	$\frac{\cos^2(\theta)}{m_l}+\frac{\sin^2(\theta)}{m_t}$	$\frac{\cos^2(\theta)}{m_t}+\frac{\sin^2(\theta)}{m_l}$	$\frac{1}{m_t}$
w_2	$\frac{1}{r}\left(\frac{\sin^2(\theta)}{m_l}+\frac{\cos^2(\theta)}{m_t}\right)$	$\frac{1}{r}\left(\frac{\sin^2(\theta)}{m_t}+\frac{\cos^2(\theta)}{m_l}\right)$	$\frac{1}{r\,m_t}$
w_3	$\frac{2\cos(\theta)\sin(\theta)(m_l-m_t)}{r\,m_t m_l}$	$\frac{2\cos(\theta)\sin(\theta)(m_t-m_l)}{r\,m_t m_l}$	0
w_4	$\frac{2\cos(\theta)\sin(\theta)(m_t-m_l)}{r^2\,m_t m_l}$	$\frac{2\cos(\theta)\sin(\theta)(m_l-m_t)}{r^2\,m_t m_l}$	0
w_5	$\frac{1}{r^2}\left(\frac{\sin^2(\theta)}{m_l}+\frac{\cos^2(\theta)}{m_t}\right)$	$\frac{1}{r^2}\left(\frac{\sin^2(\theta)}{m_t}+\frac{\cos^2(\theta)}{m_l}\right)$	$\frac{1}{r^2 m_t}$
m_x	m_t	m_t	m_l

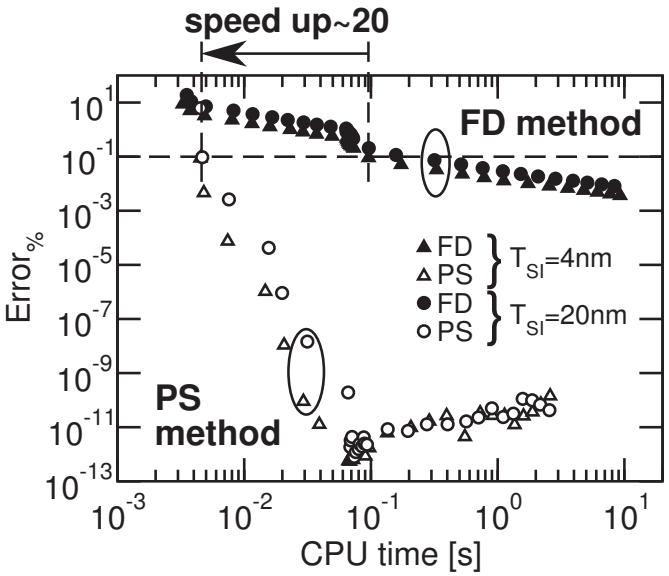

Fig. 1. (001)-hole inversion layer with a **k·p** model for a square well confining potential with different widths T_{SI}: maximum relative error versus the CPU time for the 10 lowest subbands for the PS and the FD methods. The speed-up given by the PS method over the FD one at a relative error of 0.1% is indicated.

IV. SIMULATION RESULTS

The solutions of the three Schrödinger problems obtained with either the PS or the FD methods have been first compared by using ideal quantum wells (i.e. with constant potential energy inside the well). Indeed, in this case the exact solutions for the eigenvalues are known and they have been used as reference in order to evaluate the accuracy of the numerical methods. Figs.1 and 2 show the results for the 1D **k·p** quantization problem; Fig.1 illustrates the remarkable speed-up of the PS with respect to the FD method for a given accuracy and Fig.2 shows that a much larger number of points is necessary in the FD method in order to obtain a good description of the wave-function. This is due to the spectral accuracy achieved by the PS method, which results in a dramatic improvement

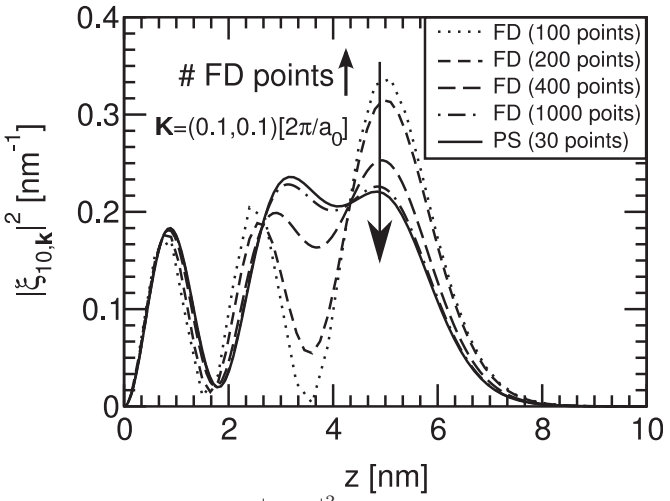

Fig. 2. Squared magnitude $|\xi_{10,\mathbf{k}}|^2$ of the tenth wave-function of the $\mathbf{k}\cdot\mathbf{p}$ problem calculated with the PS and the FD methods for a triangular confining potential with F_z=1MV/cm and k_x=k_y=0.1 $[2\pi/a_0]$.

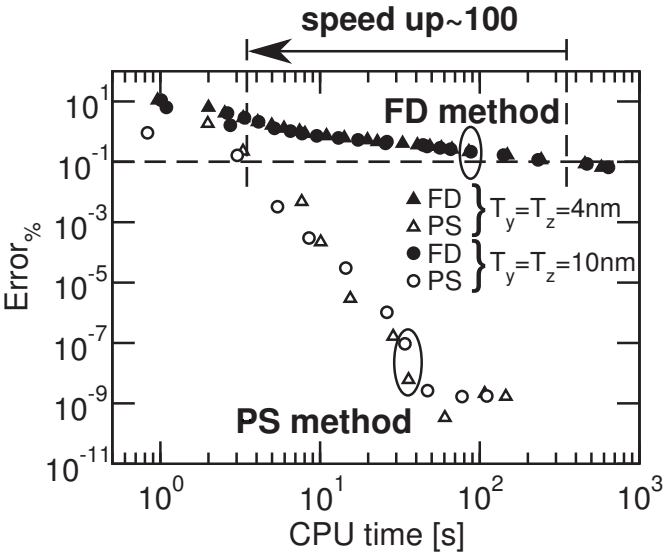

Fig. 3. Two-dimensional EMA Schrödinger problem: maximum relative error versus the CPU time for the 10 lowest subbands for the PS and the FD methods in an ideal square well.

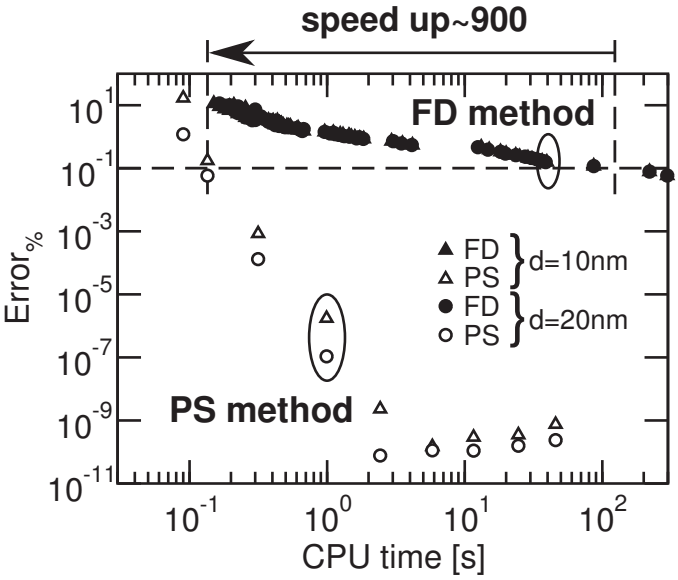

Fig. 4. Two-dimensional EMA Schrödinger problem: maximum relative error versus the CPU time for the 10 lowest subbands for the PS and the FD methods in an ideal circular well.

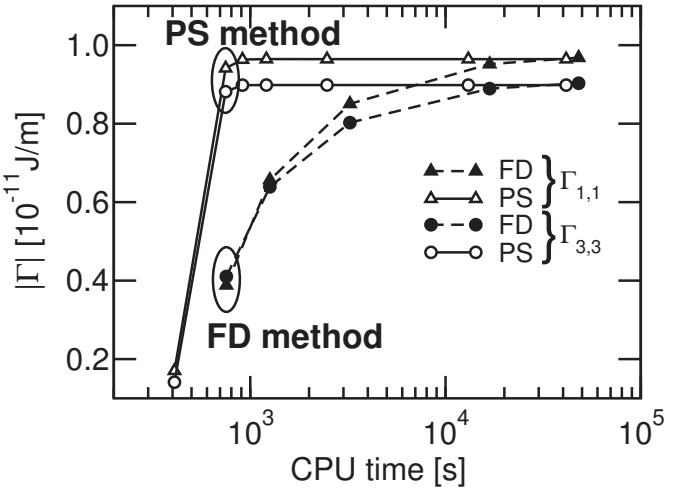

Fig. 5. Self-consistent solution of the $\mathbf{k}\cdot\mathbf{p}$-Poisson problem for a (001)-hole inversion layer (inversion density $P_{inv}\approx 6\times10^{12}\mathrm{cm}^{-2}$): surface roughness intra-subband matrix element $\Gamma_{i,j}$ [7] versus the CPU time calculated with either the PS or the FD methods.

of the numerical efficiency with respect to the FD method, whose error decreases only as N^{-2} (not shown). We can also assert that, in general, the larger is the domain, the higher is the speed-up (not shown).

Figs.3 and 4 confirm that also for the 2D Schrödinger problem in an ideal square or circular well the PS method results in a remarkable improvement in CPU time with respect to the FD method.

In the electron device modelling the refinement of the discretization grid is frequently imposed by the precision necessary to determine some physically relevant quantities. For the mobility simulation in p-MOSFETs, for example, the calculation of the surface roughness matrix elements $\Gamma_{i,j}$ may be challenging, because they are related to the first derivative of the wave-functions at the semiconductor-oxide interface [7]. In this respect, Fig.5 shows that the PS method reaches a stable value for $\Gamma_{i,j}$ with a CPU time almost a hundred times smaller than the FD method.

As for the cylindrical nanowires described by Eq.6, Fig.6 shows the equilibrium electron concentration $n(r,\theta)$ for a diameter d=10nm. Quite interestingly $n(r,\theta)$ is *not independent* of θ in the quantization plane, which confirms that, as said above, Eq.6 does not imply any radial symmetry. For the valleys ν=1,2 of Tab.I, several works [10], [11] solved Eq.6 by using circular bands with an isotropic effective mass m_{iso}=$(2m_tm_l)/(m_t+m_l)$, resulting in a radial symmetry that simplifies the numerical solution of Eq.6 (as in the case ν=3 in Tab.I). Fig.6 shows that this approximation may not be always reliable; indeed we have also verified that, for a given N_{inv}, the eigenvalues obtained with the isotropic approximation of Eq.6 can differ significantly from the exact eigenvalues, except

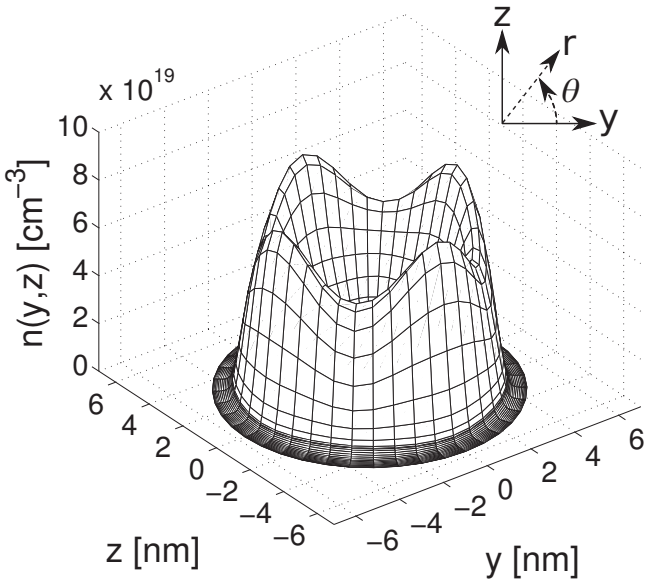

Fig. 6. Electron concentration $n(y,z)$ simulated with the PS method for a d=10nm cylindrical nanowire with an oxide thickness EOT=0.7nm at $N_{inv} \approx 3.1 \times 10^7 \mathrm{cm}^{-1}$. The electron concentration is clearly anisotropic.

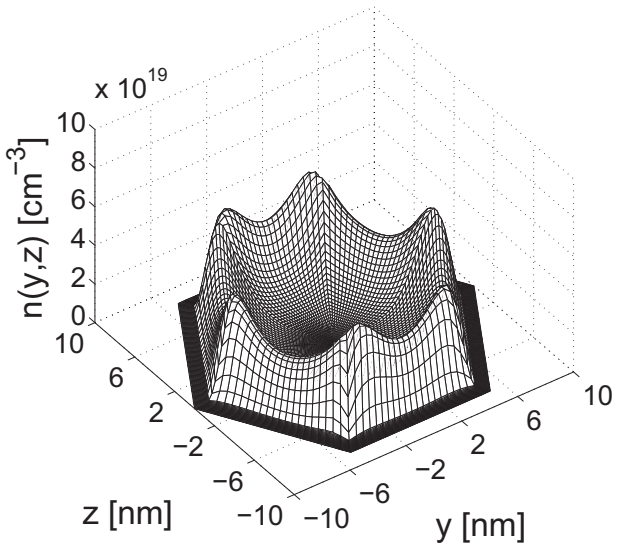

Fig. 7. Electron concentration $n(y,z)$ obtained from the solution of the self-consistent Schrödinger-Poisson problem for a hexagonal geometry with EOT=1nm at $N_{inv} \approx 3.7 \times 10^7 \mathrm{cm}^{-1}$ using PS method.

for very small diameters below 3nm (not shown).

The PS method is overall a robust numerical approach and we used it to develop also a Schrödinger-Poisson solver for nanowires with sections of fairly arbitrary shape; as an example, Fig.7 shows the electron concentration $n(y,z)$ obtained in a hexagonal domain.

V. Conclusion

This paper has investigated quantitatively the numerical efficiency of the PS versus the standard FD method for the modelling of quantization effects in nanoscale MOS transistors. In all the cases we observed a remarkable advantage of the PS compared to the FD method in terms of CPU time.

Acknowledgement

The authors would like to thank Prof. L. Selmi and P. Palestri for helpful discussions and for promoting the inter-departmental collaboration at the origin of this work. This work was supported in part by the EU (NANOSIL NoE No. IST-216171) and by the project ENIAC.JTI–MODERN.

References

[1] Q. H. Liu, C. Cheng, and H. Massoud, "The Spectral Grid Method: a Novel Fast Schrödinger-Equation Solver for Semiconductor Nanodevice Simulation," *IEEE Trans. on Computer-Aided Design of Integrated Circuits and Systems*, vol. 23, no. 8, pp. 1200–1208, Aug. 2004.

[2] C. Cheng, Q. H. Liu, J.-H. Lee, and H. Z. Massoud, "Spectral Element Method for the Schrödinger-Poisson System," *Journal of Computational Electronics*, vol. 3, pp. 417–421, 2004.

[3] J.-H. Lee and Q. H. Liu, "An Efficient 3-D Spectral-Element Method for Schrödinger Equation in Nanodevice Simulation," *IEEE Trans. on Computer-Aided Design of Integrated Circuits and Systems*, vol. 24, pp. 1848–1858, 2005.

[4] C. Cheng, J.-H. Lee, H. Z. Massoud, and Q. H. Liu, "3-D Self-Consistent Schrödinger-Poisson Solver: the Spectral Element Method," *Journal of Computational Electronics*, vol. 7, pp. 337–341, 2008.

[5] L. N. Trefethen, *Spectral Methods in MATLAB*. SIAM, Philadelphia, USA, 2000.

[6] P. J. Davis, *Interpolation & Approximation*. Dover, New York, USA, 1975.

[7] M. V. Fischetti, Z. Ren, P. M. Solomon, M. Yang, and K. Rim, "Six-band $\mathbf{k} \cdot \mathbf{p}$ Calculation of the Hole Mobility in Silicon Inversion Layers: Dependence on Surface Orientation, Strain, and Silicon Thickness," *Journal of Applied Physics*, vol. 94, no. 2, pp. 1079–1095, 2003.

[8] D. Esseni, F. Conzatti, M. De Michielis, N. Serra, P. Palestri, L. Selmi, "Semi-classical Transport Modelling of CMOS Transistors with Arbitrary Crystal Orientations and Strain Engineering," *Journal of Computational Electronics*, vol. 8, pp. 209–224, 2009.

[9] M. Bescond, N. Cavassilas, and M. Lannoo, "Effective-mass Approach for n-type Semiconductor Nanowire MOSFETs Arbitrarily Oriented," *Nanotechnology*, vol. 18, no. 25, p. 255201 (6pp), 2007.

[10] A. Marchi, E. Gnani, S. Reggiani, M. Rudan, and G. Baccarani, "Investigating the Performance Limits of Silicon-nanowire and Carbon-nanotube FETs," *Solid-State Electronics*, vol. 50, no. 1, pp. 78 – 85, 2006.

[11] S. Jin, M. V. Fischetti, and T. wei Tang, "Modeling of Electron Mobility in Gated Silicon Nanowires at Room Temperature: Surface Roughness Scattering, Dielectric Screening, and Band Nonparabolicity," *Journal of Applied Physics*, vol. 102, no. 8, p. 083715, 2007.